

A new model for NVSS galaxy catalogue using the redshift distribution and the halo minimum mass

A. Marcos-Caballero^{1,2*}, P. Vielva¹, E. Martínez-González¹, F. Finelli^{3,4},
A. Gruppuso^{3,4} and F. Schiavon^{3,4}

¹*Instituto de Física de Cantabria (CSIC - Univ. Cantabria), Av. de Los Castros s/n, E-39005 - Santander, Spain*

²*Departamento de Física Moderna (Univ. Cantabria), Av. de Los Castros s/n, E-39005 - Santander, Spain*

³*INAF-IASF Bologna, Istituto di Astrofisica Spaziale e Fisica Cosmica di Bologna, Via Gobetti 101, I-40129 Bologna, Italy*

⁴*INFN, Sezione di Bologna, Via Bertini Pichat 6/2, I-40127 Bologna, Italy*

Accepted ????. Received ???; in original form 10 November 2018

ABSTRACT

In the present paper we study the radio sources in the NRAO VLA SKY Survey (NVSS) analysing its power spectrum and galaxy distribution. There is a discrepancy between the theoretical models in the literature and the data at large scales. A new model for NVSS is proposed combining the power spectrum data from NVSS and the galaxy distribution from the Combined EIS-NVSS Survey Of Radio Sources (CENSORS). Taken into account these two data sets the differences in the power spectrum at large scales are reduced, but there is still some tension between the two data sets. Different models are compared using Bayesian evidence. A model for the galaxy distribution based on a gamma function provides a higher evidence against other models proposed in the literature. In addition, the effect of primordial non-Gaussianity has been also considered. The $2\text{-}\sigma$ constraints on the local non-Gaussian f_{NL} parameter are $-43 < f_{\text{NL}} < 142$.

Key words: – cosmology

1 INTRODUCTION

The large-scale structure (LSS) of the universe is one of the most important tools in modern cosmology, in particular, to probe the physics of the very early universe. Galaxy surveys help us to trace current matter density perturbations, which are directly related to the initial curvature perturbations. The statistical properties of these perturbations (e.g., the power spectrum and the probability distribution) are directly determined by the specific inflationary model responsible for the exponential growth of the initial perturbations (see, e.g., Liddle & Lyth 2000).

The standard paradigm of cosmic inflation predicts that the initial perturbations are near scale-invariant and Gaussianly distributed. This simplest model is confirmed by the current observations of the cosmic microwave background (CMB, Planck Collaboration et al. 2013a,b). Nevertheless, some non-standard inflation scenarios are not ruled-out by current CMB measurements. It is expected that the next step-forward on constraining cosmic inflation is coming from future galaxy surveys as Euclid (Laureijs et al. 2011), J-PAS (Benítez et al. 2009), LSST (LSST Science

Collaboration et al. 2009), WFIRST (Green et al. 2012) or Big-Boss (Schlegel et al. 2009), both in terms of the power spectrum and the probability distribution of the initial perturbations. Let us remark that, despite these capabilities to constrain cosmic inflation, the major scientific goal of future surveys is focused on the study of dark energy, by exploiting the physics of the baryon acoustic oscillations (see, Amendola et al. 2013, as an example for Euclid forecasts).

This paper studies one of the most widely galaxy survey used up to date: the NRAO VLA Sky Survey (NVSS) (Condon et al. 1998). The strength of the NVSS radio galaxy catalogue comes from its large sky coverage and its relatively high redshift range. As a drawback, it does not possess individual redshift estimation of the sources, but just a statistical description. These characteristics make NVSS a suitable catalogue (from the cosmological point of view) for cross-correlation studies with the CMB, and, also, to constrain the probability distribution of the initial perturbations.

Regarding the former analyses, it is worth mentioning that NVSS was cross-correlated with WMAP (Larson et al. 2011) to report the first detection of the integrated Sachs-Wolfe (ISW) effect Boughn & Crittenden (2004). Many subsequent analyses (e.g., Vielva et al. 2006; Pietrobon et al. 2006; McEwen et al. 2007; Schiavon et al. 2012; Giannan-

* E-mail: marcos@ifca.unican.es

tonio et al. 2012; Barreiro et al. 2013) further explored different aspects of this cross-correlation and, recently, it was also used to study the ISW effect on *Planck* (Planck Collaboration et al. 2013c) data (Planck Collaboration et al. 2013d). The ISW signal depends very much on the accurate description of the redshift distribution of the galaxies. In addition, the actual sensitivity to detect the ISW signal is also very much dependent on the correct modelling of the NVSS angular power spectrum (which also depends on the galaxy redshift distribution itself).

Constraining non-Gaussianity with galaxy surveys is being an active topic since the last five years (e.g., Dalal et al. 2008; Matarrese & Verde 2008; Desjacques & Seljak 2010; Xia et al. 2011; Giannantonio et al. 2013). This is a field in which NVSS has been also commonly used. Primordial non-Gaussianity introduces a modification in the two-point correlation function (or, conversely, the angular power spectrum) of dark matter halos (Dalal et al. 2008; Matarrese & Verde 2008; Desjacques & Seljak 2010). An evidence of this fact appears in the bias relation between halos and the underlying matter. For instance, the linear deterministic bias b becomes scale-dependent, and this dependence term is proportional to the amount of primordial non-Gaussianity.

From the previous discussion, it is clear that understanding the angular power spectrum and, therefore, the galaxy redshift distribution, is a necessary condition to extract useful cosmological information from NVSS. However, NVSS is known to suffer from some systematics, especially at very large scales. These systematics are mostly reflected as an excess of power at scales greater than 20 degrees (e.g., Hernández-Monteagudo 2010). The aim of this work is, precisely, to study in detail the statistical properties of NVSS, trying to explore further these incompatibilities.

The paper is organized as follows. In section 2 the theoretical framework used in this work is discussed, introducing some basic concepts. The data and their analysis are described in section 3 and 4. The results and conclusions are presented in sections 5 and 6 respectively.

2 THEORETICAL FRAMEWORK

According to the halo model, galaxies are formed inside halos and then it is important to characterize the clustering of halos in order to study the galaxy power spectrum. In next subsections it will be discussed the mass function of halos, the bias and redshift distribution of galaxies and the angular power spectrum. In the last subsection it will be introduced the effect of primordial non-Gaussianity in the LSS.

2.1 Mass function

The mass function of halos gives the number of dark matter halos with mass m per unit of volume at redshift z . Theoretical predictions of the mass function can be calculated assuming Gaussian perturbations (Press & Schechter 1974). It is useful to introduce the ν parameter representing the peak height. It depends on the redshift and the mass through the formula $\nu = \delta_c(z)/\sigma_m$, where σ_m is the variance of the linear matter perturbation smoothed at the scale given by the mass m (it is assumed a spherical top-hat filter) and $\delta_c(z)$ is the critical overdensity for the collapse. The Gaussian mass

function $n_G(m, z)$ is written in the universal form (Press & Schechter 1974):

$$n_G(m, z) = \frac{\bar{\rho}}{m} f(\nu) \frac{d\nu}{dm}. \quad (1)$$

In this expression $\bar{\rho}$ is the mean matter density of the universe and $f(\nu)$ is the multiplicity function. We adopt the Sheth & Tormen (1999) mass function where

$$f(\nu) = A \left(1 + \frac{1}{(2a\nu^2)^p} \right) \sqrt{\frac{a}{2\pi}} e^{-a\nu^2/2}. \quad (2)$$

The values for the parameters are: $a = 0.3$, $p = 0.707$ and $A = 0.322$. The parameter A is chosen such that the function $f(\nu)$ is normalised to unity. The Press & Schechter (1974) mass function is recovered when $a = 1$, $p = 0$ and $A = 1/2$.

2.2 Galaxy bias

In the Lagrangian space the overdensity of halos $\delta_h(m, z)$ of mass m is related to the matter overdensity δ through the bias relation. In the case of deterministic local linear bias the halo overdensity is $\delta_h(m, z) = b(m, z)\delta$. It is natural to think that galaxies are formed inside halos where the conditions for galaxy formation exists. The relation between halos and galaxies is not straightforward due to the complexity of the galaxy formation process. To deal with this problem the number of galaxies within a halo N_g is considered as a stochastic variable depending on the mass of the halo. The distribution of N_g is called the Halo Occupation Distribution (HOD) (Seljak 2000). If in a catalogue there are only halos of mass greater than M_{\min} then galaxy overdensity $\delta_g(z)$ is given by

$$\delta_g(z) = \frac{\int_{M_{\min}}^{\infty} dm n(m, z) \langle N_g \rangle \delta_h(m, z)}{\int_{M_{\min}}^{\infty} dm n(m, z) \langle N_g \rangle}, \quad (3)$$

where $n(m, z)$ is the halo mass function (Gaussian or non-Gaussian, depending on the case considered). The upper limit in the integrals is taken to be infinity considering that there are halos of arbitrary large mass in the sample. In practice the results are not strongly dependent on this maximum mass. The equation (3) leads to a similar formula for the galaxy bias:

$$b_g(z) = \frac{\int_{M_{\min}}^{\infty} dm n(m, z) \langle N_g \rangle b(m, z)}{\int_{M_{\min}}^{\infty} dm n(m, z) \langle N_g \rangle}. \quad (4)$$

Then we have that $\delta_g(z) = b_g(z)\delta$. The halo bias depends on the mass and the redshift of the halo. For the Gaussian bias, as well as for the mass function, the expression in Sheth & Tormen (1999) is adopted:

$$b(m, z) = 1 + \frac{1}{D(z)\sigma(m)} \left(a\nu - \frac{1}{\nu} + \frac{2p/\nu}{1 + (a\nu^2)^p} \right), \quad (5)$$

where $D(z)$ is the linear growth factor of perturbations normalised to unity at $z = 0$. The equation (4) depends on the average number of galaxies within a halo $\langle N_g \rangle$. As expected this quantity depends on the mass of the halo. We assume a power-law model (Berlind & Weinberg 2002),

$$\langle N_g \rangle = \begin{cases} 0 & \text{if } M < M_{\min} \\ (M/M_0)^\beta & \text{if } M > M_{\min} \end{cases}. \quad (6)$$

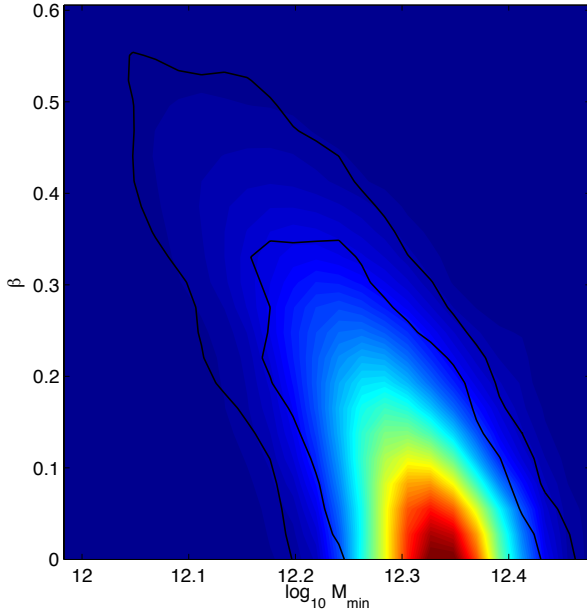


Figure 1. Parameters concerning the HOD.

The parameter β is positive definite in order to have an increasing number of galaxies with mass. In this formula the pivot of the power-law M_0 represents the mass of the halos with an average number of galaxies equal to one. The equation (4) does not depend on the parameter M_0 and then it can not be constrained using the power spectrum data. The minimum mass of halo with galaxies M_{\min} is the same as in equation (4).

2.3 Galaxy distribution and HOD

It is possible to deduce the galaxy distribution from the mass function of the halos. The mass function gives the number of halos per unit volume and mass. Multiplying the mass function by the average number of galaxies $\langle N_g \rangle$ we get the number of galaxies per redshift interval within a solid angle Ω :

$$\frac{dn}{dz} = \Omega \frac{r(z)^2}{H(z)} \int_0^\infty dm n(m, z) \langle N_g \rangle, \quad (7)$$

where $r(z)$ is the comoving distance and $H(z)$ is the hubble function. The factor before the integral is the volume per redshift interval.

The theoretical power spectrum can be completely given by the halo model and the HOD. It is possible to put constraints on the HOD parameters using the power spectrum data of NVSS. Only the minimum mass M_{\min} and the slope parameter β can be constrained using correlation functions. In Fig. 1 it is represented the posterior probability of these two parameters. With the NVSS data we only can conclude that there is not detection of the slope and the upper limit is $\beta < 0.24$ ($1-\sigma$ c.l.). For this reason in the following we will assume the slope parameter is negligible.

2.4 Galaxy angular power spectrum

In order to study two-dimensional surveys like NVSS is necessary to project the tridimensional galaxy power spectrum in the sphere. The angular power spectrum is calculated from the linear power spectrum once it is provided the redshift distribution. The galaxy angular power spectrum is given by

$$C_\ell = \frac{2}{\pi} \int dk k^2 I_\ell^2(k) P(k), \quad (8)$$

where $P(k)$ is the matter power spectrum at $z = 0$ and

$$I_\ell(k) = \int_0^\infty dz b_g(z) \frac{dn}{dz} D(z) j_\ell(k r(z)) \quad (9)$$

is the filter function of galaxies. In this expression j_ℓ are the spherical Bessel functions and $r(z)$ is the comoving distance as a function of redshift. The redshift distribution is multiplied by the galaxy bias b_g and matter overdensity growth factor $D(z)$.

2.5 Primordial non-Gaussianity

Using the Large Scale Structure (LSS) of the universe it is possible to constrain the primordial non-Gaussianity (Dalal et al. 2008; Desjacques & Seljak 2010). The nature of the primordial perturbations affects to the distribution of dark matter halos. In particular non-Gaussianity in the matter distribution modifies the two-point correlation function of halos. The bias b depends on time (or redshift), but in the case of initial Gaussian perturbations it is independent of the scale k . However the correction to the bias due to primordial non-Gaussianity is scale-dependent, and this is an important feature of the non-Gaussian bias.

In the local non-Gaussianity the potential is given by

$$\Phi(\mathbf{x}) = \phi(\mathbf{x}) + f_{\text{NL}} (\phi^2(\mathbf{x}) - \langle \phi^2 \rangle), \quad (10)$$

where the scalar ϕ is a Gaussian random field and f_{NL} is the non-linear coupling parameter which multiplies a term quadratic in ϕ . In the case that f_{NL} vanishes the potential is Gaussian. Following scalar perturbation theory the matter perturbations δ are related with the potential through the Poisson equation ($\nabla^2 \Phi \propto \delta$). In Fourier space this leads to

$$\delta_m(k, z) = \mathcal{M}_m(k, z) \Phi(k). \quad (11)$$

The perturbation field δ_m is the filtered matter perturbation field δ at a scale corresponding to halos of mass m (top-hat filter is assumed). The factor $\mathcal{M}_m(k, z)$ is

$$\mathcal{M}_m(k, z) = \frac{2}{3} \frac{k^2 T(k) D(z)}{\Omega_m H_0^2} \frac{1}{g(z = \infty)} W_m(k), \quad (12)$$

where $T(k)$ is the matter transfer function and $D(z)$ is the linear growth factor of matter normalised to unity at redshift zero. The quantity $g(z = \infty)$ is the growth suppression rate at redshift infinity. This number gives the decay of the potential in non-matter dominated universes, $\Phi(z) = g(z) \Phi(z = 0)$. It is related to the linear growth factor as $g(z) = D(z)(1 + z)$. The reason for including this term is that we are assuming the CMB convention for the f_{NL} parameter, that is, in the equation (10) all the fields are evaluated at redshift infinity. In the literature it is also used the LSS convention in which the fields are given at

redshift zero, and then this term does not appear. For the currently favoured Λ CDM model $g(z = \infty)$ has a value approximately equal to 1.4. The function $W_m(k)$ in equation (12) is the Fourier transform of the top-hat filter at scale of halos with Lagrangian mass m .

The expression for the non-Gaussian bias $b_{NG}(m, z)$ is (Matarrese & Verde 2008)

$$b_{NG}(m, z) = b(m, z) + 2f_{NL} (b(m, z) - 1) \delta_c(z) \frac{\mathcal{F}_m(k)}{\mathcal{M}_m(k, z)}, \quad (13)$$

where the scale-dependent part is proportional to f_{NL} and it is given by the factor $\mathcal{M}_m(k, z)$ in equation (12) and the function $\mathcal{F}_m(k)$. In the case of local non-Gaussianity it is

$$\mathcal{F}_m(k) = \frac{1}{8\pi^2 \sigma_m^2} \int_0^\infty dk_1 k_1^2 \mathcal{M}_m(k_1) P_\Phi(k_1) \times \int_{-1}^1 d\mu \mathcal{M}_m(k_2) \left(\frac{P_\Phi(k_2)}{P_\Phi(k)} + 2 \right), \quad (14)$$

where $k_2 = \sqrt{k^2 + k_1^2 + 2kk_1\mu}$ and $P_\Phi(k)$ is the power spectrum of the potential which is related to the matter power spectrum by $P_\Phi(k) = P_m(k, z) / [\mathcal{M}_m(k, z)]^2$.

The mass function of halos is also modified by primordial non-Gaussianity. The correction to the Gaussian mass function is given by a multiplicative factor (Matarrese et al. 2000; Lo Verde et al. 2008):

$$n_{NG}(m, z) = n_G(m, z) R(m, z), \quad (15)$$

where

$$R(m, z) = 1 + \frac{\sigma_m}{6\nu} \left[S_3 (\nu^4 - 2\nu^2 - 1) - \frac{dS_3}{d \ln \nu} (\nu^2 - 1) \right]. \quad (16)$$

In this expression S_3 is the skewness of the matter overdensity field, and then it is proportional to f_{NL} .

3 DATA

The main data used in this paper are the NVSS radio galaxies catalogue. In order to calculate the theoretical angular power spectrum it is necessary to know accurately the redshift distribution of the NVSS counts. The redshift distribution is calculated from the CENSORS data. Both are described in the next subsections.

3.1 NVSS catalogue

The NRAO VLA Sky Survey (NVSS) is a 1.4 GHz survey of the northern equatorial part of the sky up to -40° in declination (Condon et al. 1998). The most important contribution at this frequency is provided by the Active Galactic Nuclei (AGN's). One important feature of NVSS is the large sky coverage compared with other galaxy surveys. This fact allows a better estimation of the angular power spectrum.

The NVSS observations are made with two different array configurations of the radio telescopes (D and Dnc). Depending on the declination one of them is used. This fact introduces a declination systematic in the NVSS catalogue. The mean density of counts depends on the declination angle. In order to avoid this problem the NVSS sky map is corrected following the next procedure: The map is divided in declination bands with the same area. The total number of stripes in the map is 70. The mean number of counts is calculated in each stripe. This number depends on the declination due to the systematic. Then the pixels in the bands

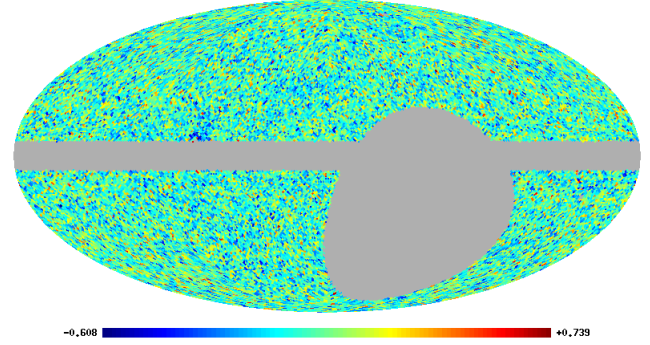


Figure 2. *Left:* NVSS map of sources with flux above 2.5 mJy. The map is at HEALPix resolution $N_{\text{side}} = 64$ (pixel size $\sim 1^\circ$).

are rescaled such that the mean number of counts in each band is equal to the full sky mean. That is,

$$n'_{ai} = \frac{\bar{n}}{\bar{n}_a} n_{ai}, \quad (17)$$

where \bar{n}_a is the mean number of counts in the band a , n_{ai} and n'_{ai} are the number of counts in the pixel i of the band a before and after the correction respectively. The mean number of counts of the full sky is represented by \bar{n} . Note that this transformation does not change the mean of the map, and the shot noise is not affected by this transformation.

The equatorial south pole from declination -40° is masked due to the absence of observations. In addition a region of width 14° around the galactic plane is also masked to avoid contamination from the Galaxy. Also some regions with high number of counts are masked with a disk of 0.6° of radius. The resulting mask is represented in Fig. 2. The fraction of observed sky is $f_{\text{sky}} = 0.73$.

We chose a flux threshold for the sources equal to 2.5 mJy. The total number of counts above this flux and outside the mask is 1.45×10^6 . It is important to have a high number of counts in order to reduce the shot noise in the estimation of the power spectrum.

3.2 CENSORS catalogue

For the modelling of the galaxy distribution of the NVSS catalogue it is used the Combined EIS-NVSS Survey Of Radio Sources (CENSORS) (Best et al. 2003; Brookes et al. 2008). This survey contains all the NVSS sources above 7.2 mJy that are within a patch of 6 deg^2 in the ESO Imaging Survey (EIS). The total number of galaxies in the survey are 149. The redshift of 44 sources are calculated using $K - z$ relation, while the remainder 103 have spectroscopic redshift (Brookes et al. 2008). With these data it is possible to estimate the redshift distribution of radio galaxies.

In the present analysis CENSORS data will be used to constrain the redshift distribution of the NVSS radio galaxies. The accurate knowledge of this distribution is important for the calculation of the angular power spectrum. The uncertainties in the estimation are taken into account performing a joint fit of the galaxy distribution and angular power spectrum at the same time. For this purpose the galaxy distribution is modelled as:

$$\frac{dn}{dz} = N \left(\frac{z}{z_0} \right)^\alpha e^{-\alpha z/z_0}. \quad (18)$$

This gamma distribution depends on two parameters, z_0 and α . The physical meaning of z_0 is the redshift at which the distribution is maximum, while α is a shape parameter. For instance, the variance of the distribution is given by $\frac{\alpha+1}{\alpha^2} z_0^2$. The constant N is chosen such that the distribution is normalised to unity. These two parameters affect both the galaxy distribution and the angular power spectrum. In Fig. 3 it is represented the CENSORS data with a fit using the gamma distribution. The best fit parameters to the CENSORS data are $z_0 = 0.53_{-0.13}^{+0.11}$ and $\alpha = 0.81_{-0.32}^{+0.34}$. In the literature there also exists a parameterization of the CENSORS galaxy distribution given in de Zotti et al. (2010):

$$\frac{dn}{dz} = 1.29 + 32.37z - 32.89z^2 + 11.13z^3 - 1.25z^4. \quad (19)$$

It is a fit to the CENSORS data using a fourth order polynomial. The units of this equation are number of counts per square degree.

4 DATA ANALYSIS

In this work we use the angular power spectrum from NVSS and the galaxy distribution given by CENSORS. In this section we describe the procedure followed in the analysis of these two data sets. Also in this section the likelihood function used to constrain the models is shown.

4.1 Angular power spectrum

The estimation of the angular power spectrum has the problem of the masked sky. The mask introduces correlations between multipoles and also affect the estimate of the power spectrum. The estimator of the angular power spectrum is given by (Hivon et al. 2002)

$$\hat{C}_\ell = \sum_{\ell' m'} M_{\ell\ell'} \frac{1}{2\ell' + 1} |a_{\ell' m'}|^2, \quad (20)$$

where the $a_{\ell m}$'s are the spherical harmonic coefficients of the masked map. The mode coupling matrix $M_{\ell\ell'}$ is

$$M_{\ell_1 \ell_2} = \frac{2\ell_2 + 1}{4\pi} \sum_{\ell_3} w_{\ell_3} \begin{pmatrix} \ell_1 & \ell_2 & \ell_3 \\ 0 & 0 & 0 \end{pmatrix}^2. \quad (21)$$

The coefficients w_ℓ are the multipoles of the angular power spectrum of the mask. For the theoretical angular power spectrum C_ℓ a Gaussian likelihood is supposed:

$$-\ln \mathcal{L} = \frac{1}{2} \sum_{\ell, \ell'} (\hat{C}_\ell - C_\ell) F_{\ell\ell'} (\hat{C}_{\ell'} - C_{\ell'}) - \frac{1}{2} \ln |F|, \quad (22)$$

where the Fisher matrix $F_{\ell\ell'}$ is the inverse of the covariance matrix of the \hat{C}_ℓ 's. The theoretical power spectrum C_ℓ as well as the Fisher matrix depend on the parameters of the model. In the case of the full sky approximation this matrix is diagonal, but in general the mask introduces couplings between multipoles. In a theoretical framework the Fisher matrix is given by (Hinshaw et al. 2003; Xia et al. 2011)

$$F_{\ell\ell'} = \frac{(2\ell + 1)M_{\ell\ell'}}{(C_\ell + N_\ell)(C_{\ell'} + N_{\ell'})}, \quad (23)$$

where the matrix $M_{\ell\ell'}$ is given by equation (21). We have verified that these estimates agree within the uncertainties

with those performed by the QML developed in Schiavon et al. (2012).

4.2 Galaxy distribution

CENSORS data are divided in redshift bins each one of width 0.2. The data cover a range of redshift from 0 to 3.6. In total there are 18 bins. The number counts in the i -th bin is denoted by \hat{n}_i . We assume that the probability distribution of the number counts in each bin is Poissonian:

$$-\ln \mathcal{L} = \sum_i (n_i - \hat{n}_i \ln n_i), \quad (24)$$

where n_i is the prediction of the model given by the galaxy distribution in equation (18). Note that we are not taking into account correlations between different bins. Possible correlations are negligible because the bin width is large compared with the galaxy correlation scale and with the typical error in redshift. Most of the galaxies have a spectroscopy error around 10^{-3} (Brookes et al. 2008).

5 RESULTS

5.1 Galaxy distributions

In this section we will examine the galaxy distributions proposed to describe the radio galaxies in the NVSS catalogue. We use the NVSS galaxy power spectrum as the data to compare the different galaxy distribution models proposed in the literature. Different methods have been used to model the NVSS sources. In Dunlop & Peacock (1990) they analyse the luminosity function of radio sources in order to determine their evolution. For this model Boughn & Crittenden (2002) proposed a constant bias model and they found the value of $b = 1.6$. In Ho et al. (2008) the NVSS source distribution is calculate using the cross-correlation between NVSS and other galaxy surveys, assuming a gamma function for the fit. In the literature a parameterization of the CENSORS data from de Zotti et al. (2010) also exists. In this case the data are fitted to a fourth order polynomial (see eqn. 19). In Fig. 3 all these models for the NVSS galaxy distribution are represented. We will perform a Bayesian evidence test comparing all these models. The galaxy distribution is fixed and the only free parameter is related to the bias. The model for the bias is given by equation (4), except for the Ho et al. (2008) galaxy distribution. In this case it is assumed a constant bias as it is suggested in that paper. The values of the evidences comparing all the models are in the Table 1. It is examined two cases: one when all the multipoles are taken into account ($\ell_{\min} = 2$) and other considering only multipoles above $\ell_{\min} = 10$. When the full set of multipoles are considered large differences between models are found, given more evidence to the ‘‘gamma model’’. However if lower multipoles are ignored the evidences are more similar. This fact could be an indication of the inconsistency of the galaxy distribution and the low- ℓ power spectrum data. In Fig. 4 it is represented the power spectra for the different models. It can be appreciated that there is a discrepancy between the models and data at large scales.

	Model	$\ln(\text{Evidence})$	$\ln(K)$
$\ell_{\min} = 2$	Gamma	1472.68	-
	de Zotti et al. (2010)	1459.15	13.53
	Ho et al. (2008)	1465.28	7.4
	Dunlop & Peacock (1990)	1463.62	9.06
$\ell_{\min} = 10$	Gamma	1412.92	-
	de Zotti et al. (2010)	1409.18	3.74
	Ho et al. (2008)	1412.12	0.8
	Dunlop & Peacock (1990)	1410.88	2.04

Table 1. Evidences for different models of the galaxy distribution taken into account the power spectrum data. The last column is the logarithm of the Bayes factor between the Gamma model and the others.

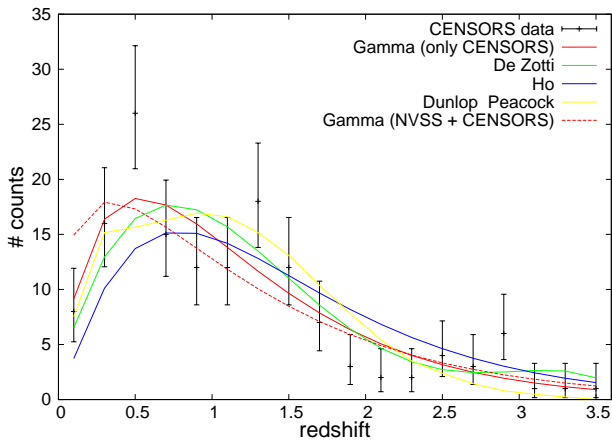


Figure 3. Galaxy distribution for different models and CENSORS data. The error bars correspond to 68% confidence level of the Poisson distribution. All distributions are normalised such that the total number counts correspond to that of CENSORS. The red lines correspond to the gamma function model. The solid line is a fit to the CENSORS data and the dashed one also takes into account the NVSS power spectrum besides CENSORS.

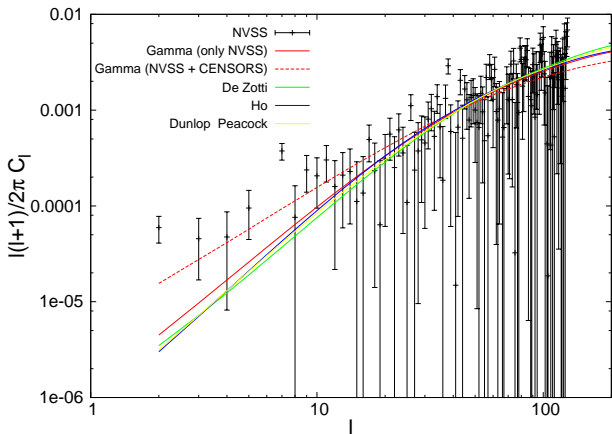


Figure 4. Angular Power spectrum of NVSS. The points with the error bars represent the power spectrum of the NVSS sources with flux above 2.5 mJy. The solid lines are different models proposed to describe the NVSS power spectrum ($\ell_{\min} = 2$). The dashed line is a joint fit to the NVSS and CENSORS assuming a gamma function model for the galaxy distribution

	Model	$\ln(\text{Evidence})$	$\ln(K)$
$\ell_{\min} = 2$	Joint fit	1436.91	-
	Gamma	1430.63	6.28
	de Zotti et al. (2010)	1415.77	21.14
	Ho et al. (2008)	1415.50	21.41
$\ell_{\min} = 10$	Dunlop & Peacock (1990)	1412.05	24.86
	Joint fit	1365.37	-
	Gamma	1370.86	-5.49
	de Zotti et al. (2010)	1365.79	-0.42
	Ho et al. (2008)	1362.35	3.02
	Dunlop & Peacock (1990)	1359.31	6.06

Table 2. Evidence for the comparison of different galaxy distribution models with the joint fit model using the power spectrum and CENSORS data. The last column is the logarithm of the bayes factor between each galaxy distribution and the joint fit.

5.2 Joint fit to NVSS and CENSORS data

It is also possible to explore the case in which the NVSS power spectrum and the CENSORS galaxy distribution are taking into account in the analysis at the same time. In this case the two data sets are supposed to be independent and the joint likelihood is the product of the likelihoods (22) and (24). For the galaxy distribution it is supposed a gamma function model (equation 18). The power spectrum also depends on the parameters affecting the galaxy distribution as well as the bias parameters. As in the previous case we assume a bias model depending on one parameter (M_{\min}) given by the equation (4). The best fit power spectrum is shown in Fig. 4.

In Table 2 it is shown the evidences of the joint fit (varying also the galaxy distribution parameters) and models with the galaxy distributions fixed. The same galaxy distributions that appear in Table 1 are considered. We can see that the results derived for the two cases considered, all multipoles and only multipoles $\ell \geq 10$, are quite different. The evidences are more similar in the first case and this is another prove that something strange is present at large scales. When all the multipoles are considered the joint fit provides much higher evidence than the other models with less number of parameters. This is a consequence of the freedom of the joint fit model to reproduce the problematic data. The parameters for this case appear in the first rows of Table 3 (Gaussian case). The redshift of the maximum of the distribution ($z_0 = 0.33$) differs from the one obtained with the CENSORS data only ($z_0 = 0.53$) and the error bars are not compatible. This fact is an evidence of some tension between the NVSS and the CENSORS data sets, possibly caused by the excess of power in the NVSS power spectrum. The increment of the number counts at low redshifts produces more power at large scales in the angular power spectrum.

5.3 Non-Gaussianity

We explore non-Gaussianity in NVSS taken into account also the CENSORS data. A joint fit of the NVSS power spectrum and the galaxy distribution provided by CENSORS is done in a scenario with primordial non-Gaussianity. The primordial non-Gaussianity is more significant at large scales and for this reason all the multipoles are included in this anal-

	Parameter	best fit	Mean	σ	ln(Evidence)
G	$\log_{10} M_{\min}$	12.66	12.63	0.19	
	z_0	0.33	0.34	0.04	1437.59 ± 0.13
	α	0.37	0.40	0.09	
NG	$\log_{10} M_{\min}$	12.52	12.44	0.20	
	z_0	0.46	0.49	0.08	1438.84 ± 0.13
	α	0.63	0.75	0.22	
	f_{NL}	54	66	40	

Table 3. Comparison of the two models with and without non-Gaussianity. Best fit and the marginalised mean value with the $1\text{-}\sigma$ errors. The last column is the evidence of each model. These values are for the full set of multipoles ($\ell \geq 2$)

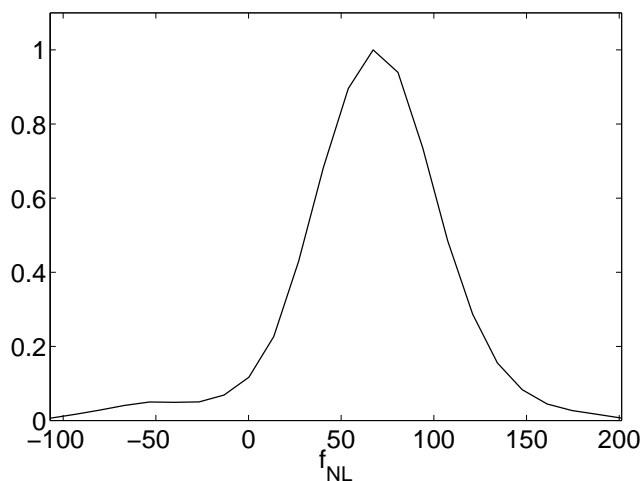


Figure 5. Marginalised likelihood for f_{NL} .

ysis. As mentioned before, primordial non-Gaussianity is a possible explanation for the excess of power at large scales.

In the Table 3 the parameters obtained with and without non-Gaussianity are summarized. In the non-Gaussian case a f_{NL} of approximately 54 is needed to fit the data. However the $2\text{-}\sigma$ constraints, $-43 < f_{\text{NL}} < 142$, are compatible with the Gaussian case ($f_{\text{NL}} = 0$) and also with the result obtained in Planck Collaboration et al. (2013b) ($f_{\text{NL}} = 2.7 \pm 5.8$). The value of f_{NL} that we find is more consistent with zero than the one obtained in Xia et al. (2010) ($25 < f_{\text{NL}} < 117$) and it is compatible with the result in Giannantonio et al. (2013) for the NVSS power spectrum. In Fig. 5 it is represented the marginalised probability of f_{NL} . Also in the last column of the Table 3 there are the evidences of both models. These numbers provide a Bayes factor $\ln(K) = 1.25$ and therefore there is no strong preference for any model. But when non-Gaussianity is taken into account the parameters of the galaxy distribution, specially z_0 (the maximum of the distribution), are compatible with the CENSORS data. Then, the tension between the NVSS and the CENSORS data sets is reduced.

6 CONCLUSIONS

In this paper we have analysed the NVSS power spectrum trying to understand the discrepancy existing between data

and the theoretical model at large scales. There are some problems concerning the NVSS data. The first of them is a declination systematic present in the number counts of NVSS due to the observation strategy of the VLA. When fainter sources are removed from the catalogue this systematic becomes less significant. We consider that the declination systematic is negligible for sources with flux above 10 mJy, but it remains for data with lower flux threshold. In order to mitigate this problem we propose a correction of the data based on the rescaling of the number of counts in declination stripes. This correction is applied to NVSS counts with flux above 2.5 mJy. When we compare the power spectra for different flux thresholds they are compatible. The advance of working with sources with a flux limit of 2.5 mJy is that the Poissonian noise is considerably reduced. Having under control the declination systematic the problem of NVSS at large scales still persists. In this work we consider different theoretical models for the NVSS galaxy distribution and all of them have problems in the power spectrum at large scales. When the large scales are removed from the analysis ($\ell \geq 10$) then all the models become compatible with the data. This fact is a direct evidence of the lack of a good modelling of NVSS at large scales.

There are different possible explanations for excess of power at large scales. It could be an unexplained systematic in the NVSS data. In the present work we rule out the declination systematic as the origin of this excess. Another possibility is that the origin of the excess is fundamental. A well known mechanism which contributes to the power spectrum at large scales is the primordial non-Gaussianity. We have also tested the possibility that primordial non-Gaussianity could explain the power excess. The value inferred for f_{NL} has a large error bar and it is compatible with zero at the $2\text{-}\sigma$ confidence level. For values of f_{NL} compatible with the Planck constraints (Planck Collaboration et al. 2013b) the effect on the fit of the data is negligible.

ACKNOWLEDGMENTS

We acknowledge partial financial support from the Spanish *Ministerio de Economía y Competitividad* Projects AYA2010-21766-C03-01, AYA2012-39475-C02-01 and Consolider-Ingenio 2010 CSD2010-00064. The authors acknowledge the computer resources, technical expertise and assistance provided by the *Spanish Supercomputing Network* (RES) node at Universidad de Cantabria.

REFERENCES

- Amendola L., Appleby S., Bacon D., Baker T., Baldi M., Bartolo N., Blanchard A., Bonvin C., et al. 2013, *Living Reviews in Relativity*, 16, 6
- Barreiro R. B., Vielva P., Marcos-Caballero A., Martínez-González E., 2013, *MNRAS*, 430, 259
- Benítez N., Gaztañaga E., Miquel R., Castander F., Moles M., Crocce M., Fernández-Soto A., Fosalba P., et al. 2009, *ApJ*, 691, 241
- Berlind A. A., Weinberg D. H., 2002, *ApJ*, 575, 587
- Best P. N., Arts J. N., Röttgering H. J. A., Rengelink R., Brookes M. H., Wall J., 2003, *MNRAS*, 346, 627

- Boughn S., Crittenden R., 2004, *Nature*, 427, 45
- Boughn S. P., Crittenden R. G., 2002, *Physical Review Letters*, 88, 021302
- Brookes M. H., Best P. N., Peacock J. A., Röttgering H. J. A., Dunlop J. S., 2008, *MNRAS*, 385, 1297
- Condon J. J., Cotton W. D., Greisen E. W., Yin Q. F., Perley R. A., Taylor G. B., Broderick J. J., 1998, *AJ*, 115, 1693
- Dalal N., Doré O., Huterer D., Shirokov A., 2008, *Phys. Rev. D*, 77, 123514
- de Zotti G., Massardi M., Negrello M., Wall J., 2010, *A&A Rev.*, 18, 1
- Desjacques V., Seljak U., 2010, *Advances in Astronomy*, 2010
- Dunlop J. S., Peacock J. A., 1990, *MNRAS*, 247, 19
- Giannantonio T., Crittenden R., Nichol R., Ross A. J., 2012, *MNRAS*, 426, 2581
- Giannantonio T., Ross A. J., Percival W. J., Crittenden R., Bacher D., Kilbinger M., Nichol R., Weller J., 2013, *ArXiv e-prints*
- Green J., Schechter P., Baltay C., Bean R., Bennett D., Brown R., Conselice C., Donahue M., et al. 2012, *ArXiv e-prints*
- Hernández-Monteagudo C., 2010, *A&A*, 520, A101
- Hinshaw G., Spergel D. N., Verde L., Hill R. S., Meyer S. S., Barnes C., Bennett C. L., Halpern M., Jarosik N., Kogut A., Komatsu E., Limon M., Page L., Tucker G. S., Weiland J. L., Wollack E., Wright E. L., 2003, *ApJS*, 148, 135
- Hivon E., Górski K. M., Netterfield C. B., Crill B. P., Prunet S., Hansen F., 2002, *ApJ*, 567, 2
- Ho S., Hirata C., Padmanabhan N., Seljak U., Bahcall N., 2008, *Phys. Rev. D*, 78, 043519
- Larson D., Dunkley J., Hinshaw G., Komatsu E., Nolte M. R., Bennett C. L., Gold B., Halpern M., et al. 2011, *ApJS*, 192, 16
- Laureijs R., Amiaux J., Arduini S., Auguères J., Brinchmann J., Cole R., Cropper M., Dabin C., et al. 2011, *ArXiv e-prints*
- Liddle A. R., Lyth D. H., 2000, *Cosmological Inflation and Large-Scale Structure*
- Lo Verde M., Miller A., Shandera S., Verde L., 2008, *J. Cosmology Astropart. Phys.*, 4, 14
- LSSST Science Collaboration Abell P. A., Allison J., Anderson S. F., Andrew J. R., Angel J. R. P., Armus L., Arnett D., et al. 2009, *ArXiv e-prints*
- Matarrese S., Verde L., 2008, *ApJ*, 677, L77
- Matarrese S., Verde L., Jimenez R., 2000, *ApJ*, 541, 10
- McEwen J. D., Vielva P., Hobson M. P., Martínez-González E., Lasenby A. N., 2007, *MNRAS*, 376, 1211
- Pietrobon D., Balbi A., Marinucci D., 2006, *Phys. Rev. D*, 74, 043524
- Planck Collaboration Ade P. A. R., Aghanim N., Armitage-Caplan C., Arnaud M., Ashdown M., Atrio-Barandela F., Aumont J., Baccigalupi C., Banday A. J., et al. 2013c, *ArXiv e-prints*
- Planck Collaboration Ade P. A. R., Aghanim N., Armitage-Caplan C., Arnaud M., Ashdown M., Atrio-Barandela F., Aumont J., Baccigalupi C., Banday A. J., et al. 2013d, *ArXiv e-prints*
- Planck Collaboration Ade P. A. R., Aghanim N., Armitage-Caplan C., Arnaud M., Ashdown M., Atrio-Barandela F., Aumont J., Baccigalupi C., Banday A. J., et al. 2013a, *ArXiv e-prints*
- Planck Collaboration Ade P. A. R., Aghanim N., Armitage-Caplan C., Arnaud M., Ashdown M., Atrio-Barandela F., Aumont J., Baccigalupi C., Banday A. J., et al. 2013b, *ArXiv e-prints*
- Press W. H., Schechter P., 1974, *ApJ*, 187, 425
- Schiavon F., Finelli F., Gruppuso A., Marcos-Caballero A., Vielva P., Crittenden R. G., Barreiro R. B., Martínez-González E., 2012, *MNRAS*, 427, 3044
- Schlegel D. J., Bebek C., Heetderks H., Ho S., Lampton M., Levi M., Mostek N., Padmanabhan N., Perlmutter S., et al. 2009, *ArXiv e-prints*
- Seljak U., 2000, *MNRAS*, 318, 203
- Sheth R. K., Tormen G., 1999, *MNRAS*, 308, 119
- Vielva P., Martínez-González E., Tucci M., 2006, *MNRAS*, 365, 891
- Xia J.-Q., Baccigalupi C., Matarrese S., Verde L., Viel M., 2011, *J. Cosmology Astropart. Phys.*, 8, 33
- Xia J.-Q., Viel M., Baccigalupi C., De Zotti G., Matarrese S., Verde L., 2010, *ApJ*, 717, L17

This paper has been typeset from a \TeX / \LaTeX file prepared by the author.